An Investigation Into Thermal Bridging Effects in an Envelope Integrated With End-Of-Life Photovoltaic Panels

Roshan Raghavendra Rao – Indian Institute of Science, India – roshanrao@iisc.ac.in
Monto Mani – Indian Institute of Science, India – monto@iisc.ac.in

Abstract

Upcycling End-of-Life Solar Photovoltaic panels in buildings is a novel approach to manage the imminent growing problem of PV waste. The EoL-PV panels have been characterized to have a high U-value and low thermal mass. To address this issue, interventions involving tandem plywood (preferably EoL packaging plywood) have been proposed and tested through whole building simulations in our preceding studies. A typical PV panel is encased in an aluminium frame whose thermal conductivity is of two orders of magnitude higher than a PV panel. This causes thermal bridging, which must be accounted for in the U-value calculation of PV panels. In this study, the thermal bridging effect due to the aluminium frame is analysed using two-dimensional finite-element method-based tool, THERM. A rise in the U-value of around 13% has been estimated due to the presence of a frame in PV panel. To demonstrate the impact of U-value of PV panel on the building's thermal performance, simulations have been performed with lumped-capacitance simple single zone model in TRNSYS. One of the interventions, having the highest plywood thickness in tandem to the EoL-PV panel, was the least sensitive to the thermal bridging effect on annual heating/cooling load and fared best in terms of thermal mass.

1. Introduction

The issue of the alarming rise in the End-of-Life Photovoltaic (EoL-PV) panels is surfacing worldwide. By 2050, 60 ~ 78 million tonnes of PV waste (EoL-PV Panels) are expected globally (Weckend et al., 2016). Recycling and recovery technologies are not currently economically viable (Mathur et al., 2020). Given the inherent durability of the materials comprising PV panels, a hitherto untried upcycling solution has been proposed in using EoL-PV panels as a building material. The rising need for building materials in developing countries is imminent. Most conventional building materials are industrially sourced and inherently carry a high embodied energy (Typical brick: 1.26 ~ 3 MJ/kg; Cement: 3.6 ~ 20 MJ/kg (Praseeda & Venkatarama Reddy, 2017)). EoL-PV could be a low-cost, low-embodied energy building material. While PV has been integrated as a building envelope, the challenge of integrating EoL-PV lies in examining the impact of degradation on its solar and thermal transmittance properties and assessing its climatic-response as a building envelope. Experimentally, thermal transmittance measurements for building materials are conducted in a HotBox facility, wherein the real-life specimen is subject to a steady-state temperature difference on either side. In the context of EoL-PV, thermal transmittance (U-value) measurements for the thin non-opaque specimen have been examined in our recent study (Rao et al., 2023). A full-scale PV panel (glass-backsheet crystalline silicon PV) has been tested in a state-of-the-art HotBox facility. The U-values of the PV panels are estimated based on the heat flux and temperature difference in the controlled (environment) chamber. The dynamic thermal performance of the EoL-PV envelope, integrated as a façade, has been studied for a prototype structure (Fig. 1). The prototype structure was monitored real-time for its indoor air temperatures, EoL-PV surface temperatures (outdoors and indoors), and indoor globe temperature. The whole building simulations of the same building (calibrated) has been performed for different climatic zones in India. The decrement factor and time lag were found to be 1.13 ± 0.12(sd) and 1.6 min ± 11 min (sd) respectively. These values indicate that the building envelope is unable to adequately regulate indoor temperatures, due to the high thermal transmittance and low ther-

Part of
Pernigotto, G., Ballarini, I., Patuzzi, F., Prada, A., Corrado, V., & Gasparella, A. (Eds.). 2025. Building simulation applications BSA 2024. bu,press.
https://doi.org/10.13124/9788860462022

mal mass of the EoL-PV. This calls for suitable interventions in the building envelope integrating EoL-PV panel, for improved thermal performance.

Fig. 1 – End-of-Life Photovoltaic panel integrated building with noticeable source of thermal bridging at the edges

The interventions involve adding another EoL-PV panel in tandem or plywood. (Fig. 2) describes the construction of the interventions.

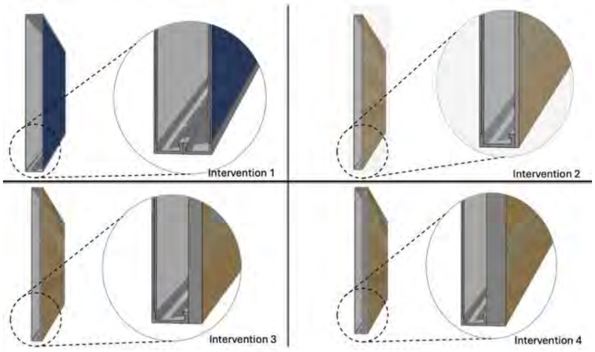

Case	Construction	Thermal mass (kJ/m^{2}K)
No intervention	EoL-PV (5mm) Panel	7
Intervention 1	EoLPV (5mm) – 100mm air – EoLPV panel (5mm)	14.1
Intervention 2	EoLPV (5mm) – 50mm air – plywood (5mm)	7.03
Intervention 3	EoLPV (5mm) – 50mm air – plywood (15mm)	21.02
Intervention 4	EoLPV (5mm) – 50mm air – plywood (30mm)	42.01

Fig. 2 – Interventions explored to improve the thermal performance of the EoL-PV envelope in a building

The scope of these studies until now was limited to the heat transfer through the EoL-PV panel without considering the effects of the aluminium frame encasing the panel. The thermal conductivity of the PV panels measured is 0.55 ~ 0.7 W/mK (Rao et al., 2023) and the aluminium is nearly two orders of magnitude higher than PV panels. When the PV panels are used as the envelope of a building in a repetitive manner, the aluminium frame can be categorized as the linear (repeating) thermal bridge (Fig. 1). As such a high thermal conductivity of the aluminium frame certainly dissipates heat faster than the PV panel, the estimation of magnitude of thermal bridging and its impact on thermal performance is important. The U-value of the EoL-PV should involve the effects of the aluminium frame. The cross section of the aluminium frame is shown in the (Fig. 3). The objective of this study is to estimate the U-values considering the thermal bridging at the aluminium frame and its impact on the overall U-value of the building. The changes in the sensible heat load of a building considering the thermal bridging are estimated.

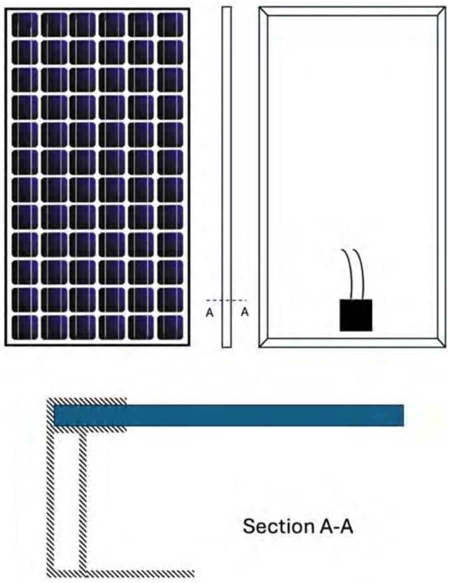

Fig. 3 – A typical commercial c-Si photovoltaic panel construction detail of the edges

The U-value of the PV panel with an aluminium frame is calculated by THERM tool (LBNL, 2023), which allows two-dimensional heat transfer using finite-element method. Previous studies (Siviour et al., 1988; Schwab et al., 2005; Boafo et al., 2015) have adopted two-dimensional heat flow analysis tools to estimate the thermal bridging effect on the envelopes. The percentage change in the U-value between ignoring and accounting for thermal bridging has been reported to parameterize the effect of thermal bridging. Further, to estimate the effect of an increased U-value on the indoor air temperature, a lumped-capacitance model is simulated in TRNSYS.

2. Methodology

2.1 Finite-Element Method for Heat Transfer Analysis (THERM)

THERM is a computer program developed at Lawrence Berkeley National Laboratory (LBNL). Using THERM, two-dimensional heat-transfer effects in building components such as windows, walls, foundations, roofs, and doors can be modelled as well as in other products where thermal bridges are of concern. THERM's heat transfer analysis is based on finite-element method, which can model complex geometries of building products. Here, the PV panels with and without a frame have been modelled for heat transfer analysis. The boundary conditions for the PV panel envelope are shown in (Fig. 4). The dimensions of the cases considered here are mentioned in (Fig. 2).

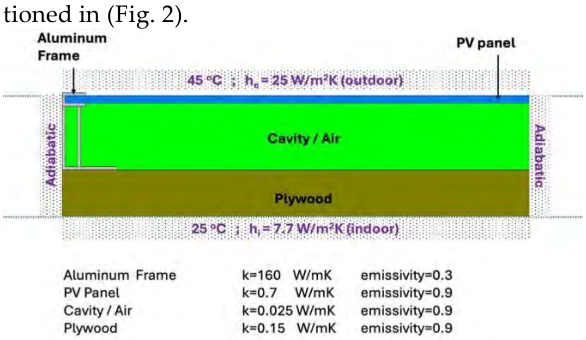

Fig. 4 – Boundary conditions applied to the heat transfer analysis in the THERM tool

Only one of the frames is analysed here as the heat flow pattern would be symmetrical along x- and y-axis. The length of the PV from frame is truncated to ~ 200 mm (total length of a typical panel is ~ 1600 mm) for analysis.

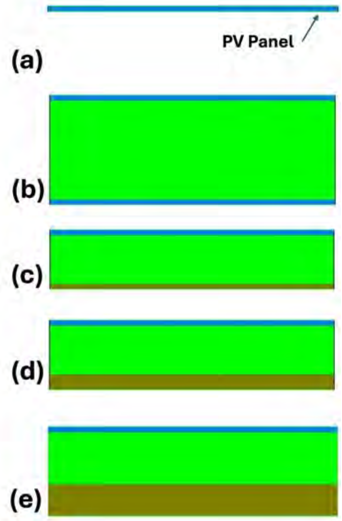

Fig. 5 – Different cases considered for heat transfer analysis without aluminum frame. (a) No intervention, (b) Intervention 1, (c) Intervention 2, (d) Intervention 3, (e) Intervention 4

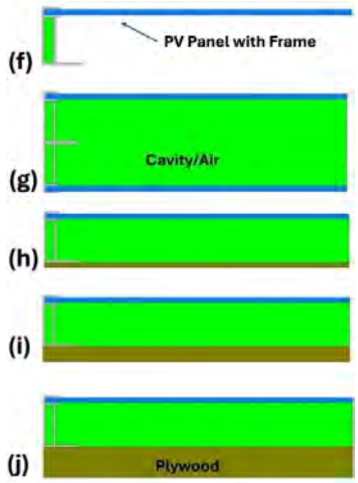

Fig. 6 – Different cases considered for heat transfer analysis with aluminum frame. (f) No intervention, (g) Intervention 1, (h) Intervention 2, (i) Intervention 3, (j) Intervention 4

The considered length is based on the development of a consistent temperature gradient beyond a critical length from the frame. The PV panels without an aluminium frame (Fig. 5) have been modelled to verify the U-values calculated by THERM with our estimations based on Hotbox measurements (Rao et al., 2023). U-values of cases (a) to (e) (Fig. 5) agree with our previous estimations. Further, to estimate the U-value accounting for thermal bridging, cases (f) to (j) (Fig. 6) have been modelled and analysed.

2.2 Lumped-Capacitance Single Zone Model (TRNSYS)

Table 1 – Cases considered for simulations using lumped-capacitance model in TRNSYS

Case	WWR	Scenario	Thermal bridging
1	10	No intervention	no bridging
2	25	No intervention	no bridging
3	40	No intervention	no bridging
4	10	Intervention 1	no bridging
5	25	Intervention 1	no bridging
6	40	Intervention 1	no bridging
7	10	Intervention 2	no bridging
8	25	Intervention 2	no bridging
9	40	Intervention 2	no bridging
10	10	Intervention 3	no bridging
11	25	Intervention 3	no bridging
12	40	Intervention 3	no bridging
13	10	Intervention 4	no bridging
14	25	Intervention 4	no bridging
15	40	Intervention 4	no bridging
16	10	No intervention	with bridging
17	25	No intervention	with bridging
18	40	No intervention	with bridging
19	10	Intervention 1	with bridging
20	25	Intervention 1	with bridging
21	40	Intervention 1	with bridging
22	10	Intervention 2	with bridging
23	25	Intervention 2	with bridging
24	40	Intervention 2	with bridging
25	10	Intervention 3	with bridging
26	25	Intervention 3	with bridging
27	40	Intervention 3	with bridging
28	10	Intervention 4	with bridging
29	25	Intervention 4	with bridging
30	40	Intervention 4	with bridging

The simple lumped-capacitance single zone model in TRNSYS has been chosen here to allow modelling an overall U value for the entire structure. It is useful to gain a comparative estimate of the heating and/or cooling load with and without accounting for heat transfer through aluminium frame. Here, the building considered is the BESTEST case 600 FF (a block of 6 m X 8 m and height of 2.7 m). The roof and walls are considered to be integrated with EoL-PV. A maximum window-wall ratio (wwr) of 40% is considered (Bureau of Energy Efficiency, 2017). Double-glazing properties (U-value of 5.1 W/m²K) are set to the floor (Bureau of Energy Efficiency, 2017). Simulations are performed for three wwr of 10%, 25% and 40%. Clay tile floor properties (U-value of 0.25 W/m²K) are set to the floor (Bureau of Energy Efficiency, 2017). The overall U value for the entire structure is calculated based on the U-values for the PV (calculated from THERM), floor, and glazing with their corresponding areas for all the 30 cases tabulated in (Table 1). The building loss coefficient (overall U-value (W/m²K)) and the building capacitance (thermal capacitance (kJ/K)) are input in TRNSYS. Other parameters like building volume, surface area and the specific heat capacity of the building air are 129 m³, 171.6 m² and 1.007 kJ/kgK respectively. The weather data of New Delhi (composite climate zone or Cwa) is used which represents a climate zone with annual maximum temperature of ~ 45 ℃ and an annual minimum of ~ 5 ℃. The indoor air temperature from the TRNSYS simulations is further analysed to estimate the sensible heating/cooling load. The simulations are run with 15 min interval for one year (8760 hours). A set temperature of 23 ℃ ~ 27 ℃ indoor are considered to estimate the sensible loads. The following expression is used to estimate the annual sensible load.

$$q = \sum_{t=0}^{t=8760\ hours} \rho V c_p \Delta T_t. \ (kJ)$$

ρ is the density of the air (1.2 kg.m³), V is the volume of the indoor air (129 m³), c_p is indoor air specific heat (1.007 kJ/kgK), ΔT_t is the difference in the set and indoor air temperature at each point.

3. Results and Discussion

The heat transfer through a PV panel without a frame is ideally one-dimensional, from the outdoor to indoor (in this study). Once accounting for the aluminum frame, a sharp drop in the temperature is seen at the frame due to higher thermal conductivity of the frame (Fig. 7). A zone of lower temperature is developed around the frame and heat transfer in the lateral direction is also seen in (Fig. 7). A uniform temperature gradient is set after a critical distance from the frame perpendicular to the gradient. The presence of another PV panel (case (b)) or plywood in (case (c-e)) creates a higher temperature gradient due to lower thermal conductivity of PV panel and plywood.

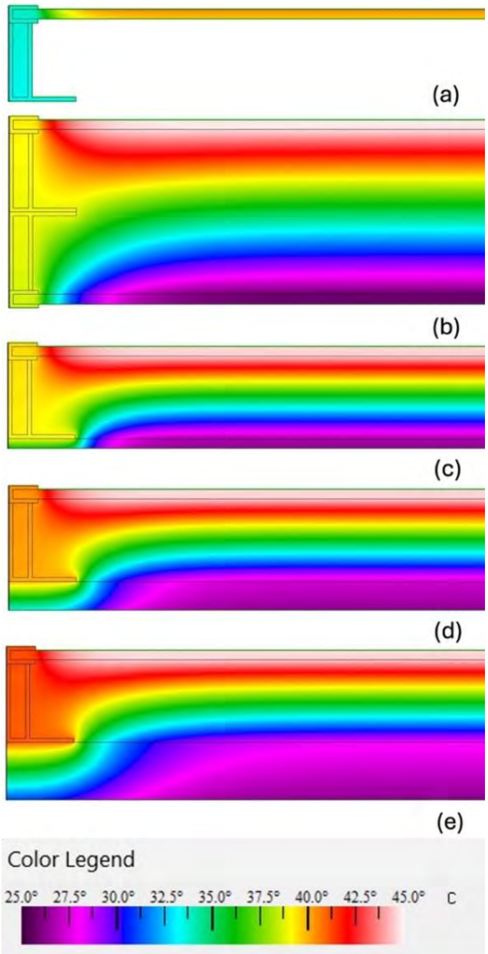

Fig. 7 – Temperature profile of the PV cross-section for different cases

Heat flux along the aluminum frame is of several orders of magnitude higher than that of the PV panels (Fig. 8). The heat flux magnitude reduced with an increase in the resistance to flow of heat by the presence of low thermal conductivity material (case b-e) (Fig. 9). The rise in the net heat transfer through the system results in higher thermal transmittance (U-value). The U-value rise on accounting for thermal bridging is tabulated in (Table 2). Ideally, to understand the impact of more frames on the sides of the panel, the percentage change needs to be multiplied by the number of frames under consideration.

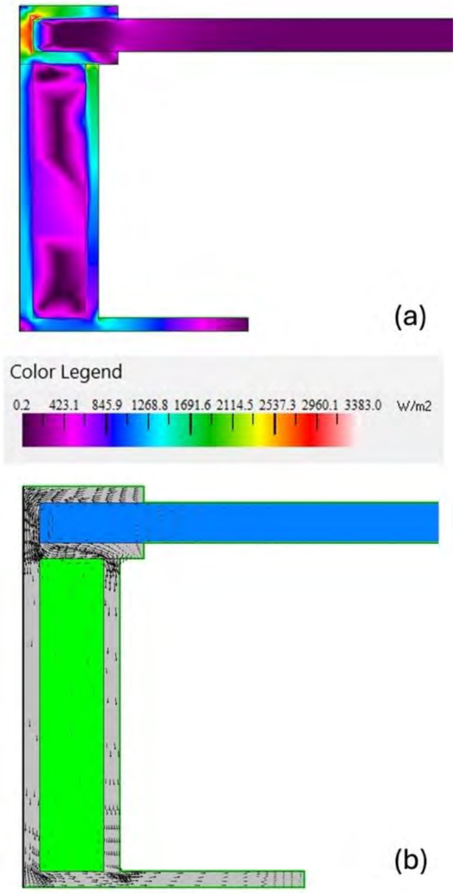

Fig. 8 – Heat flux through PV panel and the frame

The overall building U-values are calculated and are tabulated for all the cases in the (Table 3). The lumped-capacitance model was run for 30 cases (Table 1), the resulting indoor minimum and maximum air temperatures were analyzed. The effect of accounting for thermal bridging is analyzed. Thermal bridging causes the minimum temperature reached in the whole year to drop further (Fig. 10) and the maximum temperature reached in the whole year to rise further (Fig. 11). This phenomenon is consistently observed in all the cases (interventions and window-wall ratios). Amongst the cases, intervention 1, consisting of the EoL-PV panels in tandem back-to-back with a 100 mm air cavity induces maximum change in the indoor temperatures.

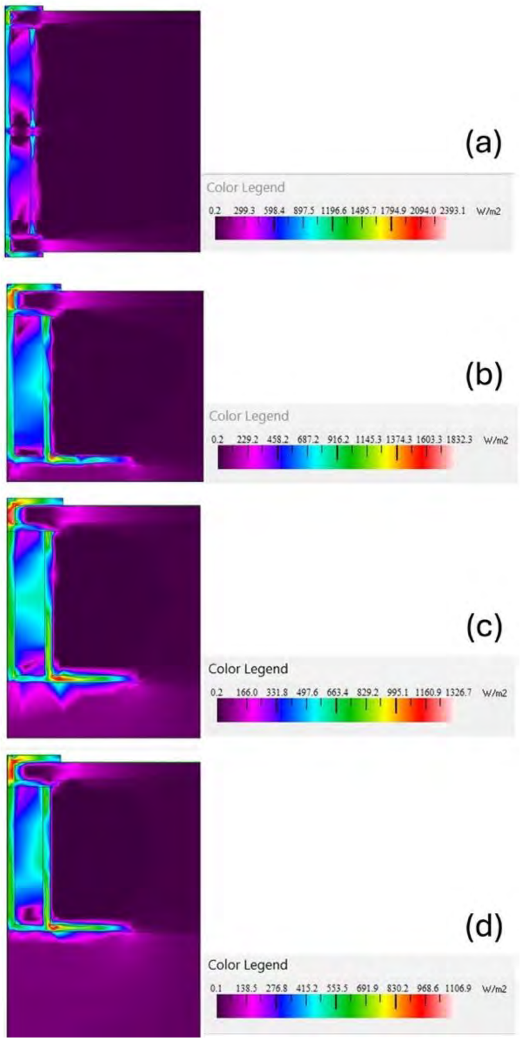

Fig. 9 – Heat flux through PV panel and the frame for the four interventions

Table 2 – The U values of EoL-PV envelopes with and without thermal bridging effect

Case	U value (W/m^2K) No thermal bridge	With thermal bridge	Change (%)
No intervention	5.6	6.35	+ 13.4
Intervention 1	0.23	0.89	+ 286.9
Intervention 2	0.45	1.07	+ 137.7
Intervention 3	0.43	0.95	+ 120.9
Intervention 4	0.42	0.83	+ 97.6

This widening in the maximum and minimum indoor temperature ranges leads to an increase in the sensible heating/cooling load as the temperature difference between the set temperature and the indoor air temperature rises. The percentage change in the annual sensible heating/cooling load for three set temperatures are analyzed.

Table 3 –The Overall U values of the EoL-PV integrated building with and without thermal bridging effect

WWR	Case	Overall U value (W/m^2K) No thermal bridging	With thermal bridging	Change (%)
10	No intervention	4.11	4.59	+ 11.58
25	No intervention	4.08	4.51	+ 10.55
40	No intervention	4.04	4.43	+ 9.49
10	Intervention 1	0.46	0.90	+ 97.48
25	Intervention 1	0.78	1.18	+ 51.61
40	Intervention 1	1.10	1.46	+ 32.57
10	Intervention 2	0.60	1.02	+ 70.04
25	Intervention 2	0.91	1.29	+ 41.81
40	Intervention 2	1.21	1.55	+ 27.86
10	Intervention 3	0.59	0.94	+ 59.05
25	Intervention 3	0.90	1.21	+ 35.04
40	Intervention 3	1.21	1.49	+ 23.27
10	Intervention 4	0.58	0.86	+ 48.23
25	Intervention 4	0.89	1.14	+ 28.37
40	Intervention 4	1.20	1.42	+ 18.76

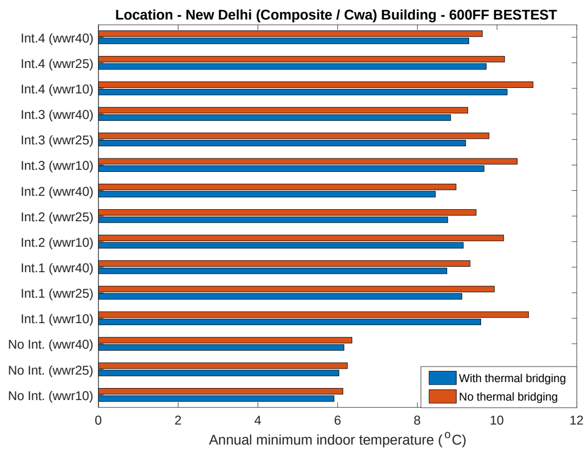

Fig. 10 – Annual minimum indoor air temperature with and without thermal bridging effects

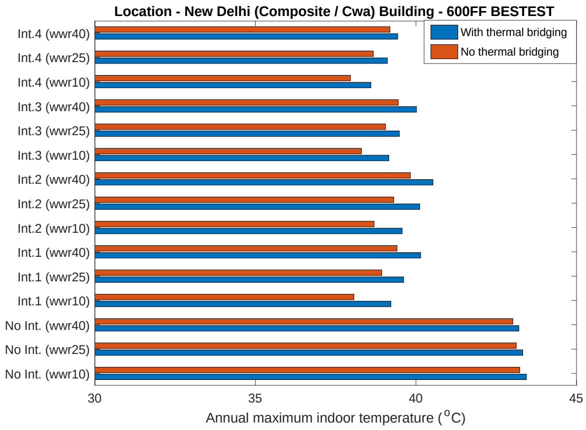

Fig. 11 – Annual maximum indoor air temperature with and without thermal bridging effects

A maximum of ~1.2% increase in the sensible heating/cooling load is seen for the considered building (Fig. 12, Fig. 13, Fig. 14). Higher window-wall ratio implies lesser area of PV panels and results in lesser contribution of thermal bridging as well. A low percentage change in the heating/cooling load is observed in intervention 4 consistently. This translates to lesser thermal bridging effects in intervention 4. This is due to a 30 mm thick layer of plywood in tandem with PV panel, which dilutes the thermal bridging effect.

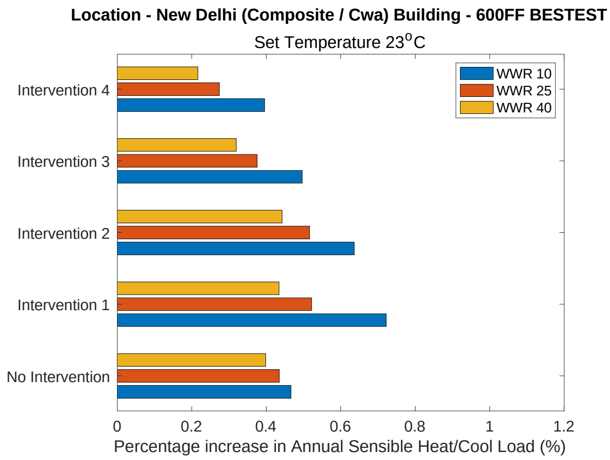

Fig. 12 – Increase in the annual sensible heating/cooling load for set temperature 23 ˚C

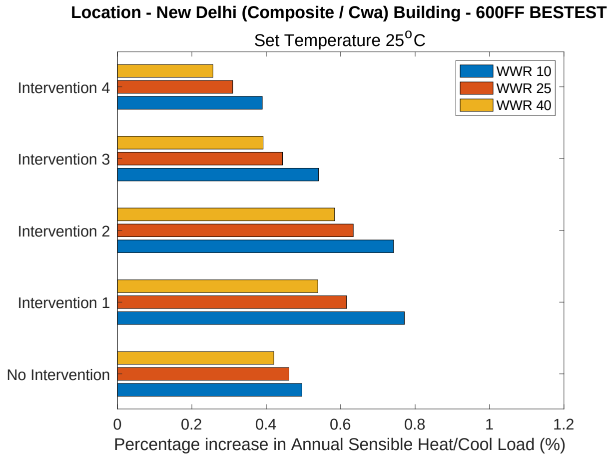

Fig. 13 – Increase in the annual sensible heating/cooling load for set temperature 25 ˚C

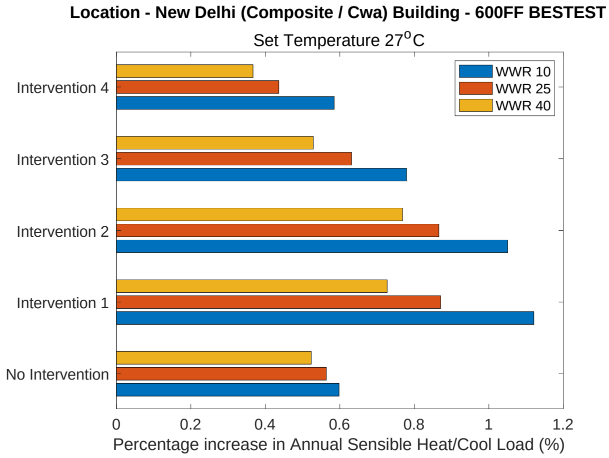

Fig. 14 – Increase in the annual sensible heating/cooling load for set temperature 27 ˚C

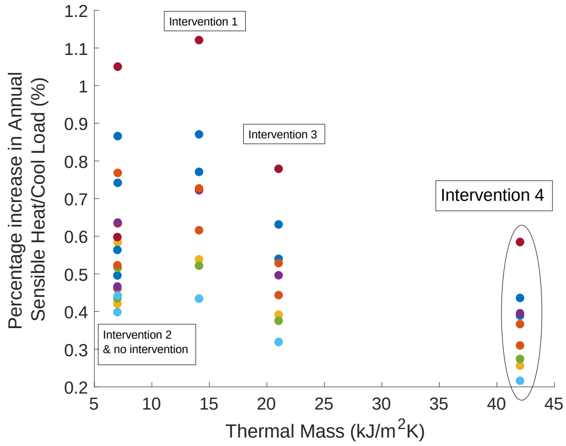

Fig. 15 – Desirable intervention considering thermal mass and thermal bridging effects

On comparing the interventions in terms of desired thermal mass and thermal bridging effect, it is seen that intervention 4 fares best in both criteria. The desirable region in the (Fig. 15) is higher thermal mass and lower percentage increase in sensible heating/cooling load. This optimum region is achieved by intervention 4. One of the strategies to avoid thermal bridging is to add an insulation layer to the envelope which is naturally designed in intervention 4 to address the low thermal mass issue. The 30 mm thick plywood serves as a common solution to improve thermal mass and reduce thermal bridging effects.

4. Conclusion

Thermal bridging effects in the envelope integrated with EoL-PV panels are studied through two-dimensional heat transfer modelling in THERM tool. The thermal bridging effects on the U-values of different intervention cases are calculated. In the case of an EoL-PV panel, around a 13% increase in the U-value is expected. The effect on the building's heating/cooling loads is dependent on various factors including thermal bridges. Here, a simple demonstration of the thermal bridging effects on a simple block is considered. Out of all the cases, intervention 4 seems to be a promising choice having a higher thermal mass and lower effect of thermal bridging due to high plywood thickness. The analysis considering the effects of all the frame around the PV panel is the scope of further studies. The role of climate zone, building type, humidity, corrosion or degradation in aluminium over time and heat capacity of the aluminium frame have not been considered here and adds to the scope of studies ahead.

Nomenclature

Symbols

q	Annual sensible heating/cooling load
ρ	Density of air
V	Volume of the indoor air
c_p	Specific heat capacity of air
ΔT_t	Difference between set and air temperature

References

Boafo, F. E., Ahn, J. G., Kim, J. T. and Kim, J. H., Computing Thermal Bridge of VIP in Building Retrofits Using DesignBuilder, *Energy Procedia*, vol. 78, pp. 400–405, 2015 http://dx.doi.org/10.1016/j.egypro.2015.11.683

Bureau of Energy Efficiency, Energy Conservation Building Code for Residential Buildings (Part I: Building Envelope Design), *ECBC*, 2017 https://beeindia.gov.in/sites/default/files/BEE_ECBC%202017.pdf

Therm 7, Windows & Daylighting. Accessed October 23, 2024. https://windows.lbl.gov/therm-78-windows-78

Mathur, D., Gregory, R. and Simmons, T., End-of-Life Management of Solar PV Panels, 2020. https://ris.cdu.edu.au/ws/portalfiles/portal/57428020/EOLManagementSolarPV_Final_e_version.pdf

Praseeda, K. I. , B V Venkatarama Reddy, M. M., Life-Cycle Energy Assessment in Buildings: Framework, Approaches, and Case Studies, *Encyclopedia of Sustainable Technologies*, p. 113, 2017

Rao, Roshan. R., and Mani, Monto., Examining the applicability of End-of-Life (EoL) Photovoltaic (PV) Panels as a building material, *40th European Photovoltaic Solar Energy Conference (EUPVSEC)*, Lisbon, Portugal, 2023

Schwab, H., Stark, C., Wachtel, J., Ebert, H. P. and Fricke, J., Thermal Bridges in Vacuum-Insulated Building Façades, *Journal of Thermal Envelope and Building Science*, vol. 28, no. 4, pp. 345–55, 2005. https://doi.org/10.1177/1097196305051794

Siviour, J. B. and Mould, A. E., Thermal Bridging: Significance in U-Value Calculation, *Building Services Engineering Research & Technology*, vol. 9, no. 3, pp. 133–35, 1988. https://doi.org/10.1177/014362448800900307

Weckend, S., Wade, A., and Heath, G., End-of-Life Management: Solar Photovoltaic Panels, International Renewable Energy Agency and International Energy Agency Photovoltaic Power Systems Programme, 2016. https://www.irena.org/-/media/Files/IRENA/Agency/Publication/2016/IRENA_IEAPVPS_End-of-Life_Solar_PV_Panels_2016.pdf